Ammonia-Borane Derived BN Fragments Trapped on Bi- and Trimetallic Titanium(III) Systems

Estefanía del Horno,[a] Jesús Jover,[b,*] Miguel Mena,[a] Adrián Pérez-Redondo[a] and Carlos Yélamos[a,*]

[a]*Departamento de Química Orgánica y Química Inorgánica, Instituto de Investigación Química "Andrés M. del Río" (IQAR), Universidad de Alcalá. 28805 Alcalá de Henares-Madrid (Spain). E-mail:* carlos.yelamos@uah.es

[b]*Departament de Química Inorgànica i Orgànica, Institut de Química Teòrica i Computacional (IQTC-UB), Universitat de Barcelona, Martí i Franquès 1-11, 08028 Barcelona (Spain). E-mail:* jesus.jover@qi.ub.es

Dedicated to Prof. Dr. Antonio Otero on the occasion of his 70th birthday.

Table of Contents:

Titanium(III) complexes containing unprecedented $(NH_2BH_2NHBH_3)^{2-}$ and $\{N(BH_3)_3\}^{3-}$ bridging ligands have been isolated by treatment of the trimethyl derivative $[Ti(\eta^5-C_5Me_5)Me_3]$ with NH_3BH_3.
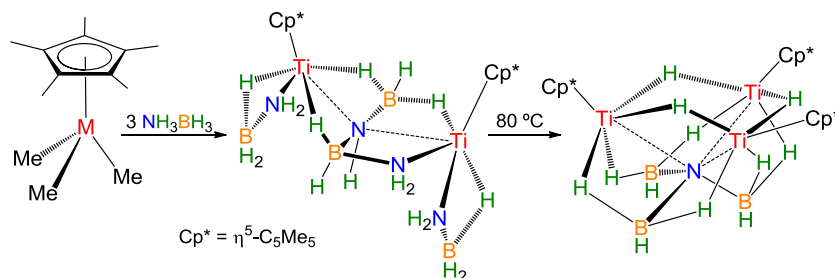
Abstract:

Titanium(III) complexes containing unprecedented $(NH_2BH_2NHBH_3)^{2-}$ and $\{N(BH_3)_3\}^{3-}$ ligands have been isolated and their structures elucidated by a combination of experimental and theoretical methods. The treatment of the trimethyl derivative $[TiCp^*Me_3]$ $(Cp^* = \eta^5\text{-} C_5Me_5)$ with NH_3BH_3 (3 equiv) at room temperature gives the paramagnetic dinuclear complex $[\{TiCp^*(NH_2BH_3)\}_2(\mu\text{-}NH_2BH_2NHBH_3)]$, which at 80 ºC leads to the trinuclear hydride derivative $[\{TiCp^*(\mu\text{-}H)\}_3\{\mu_3\text{-}N(BH_3)_3\}]$. The bonding modes of the anionic BN fragments in those complexes as well as the dimethylaminoborane group trapped on the analogous trinuclear $[\{TiCp^*(\mu\text{-}H)\}_3(\mu_3\text{-}H)(\mu_3\text{-}NMe_2BH_2)]$ have been studied by X-ray crystallography and density functional theory (DFT) calculations.

Keywords: ammonia–borane • boranes • dehydrogenation • density functional calculations • titanium

Ammonia–borane, NH_3BH_3, has been identified as one of the leading candidates for chemical hydrogen storage due to its high hydrogen content (19.6 wt %).[1] However, its thermal decomposition requires high temperatures and gives volatile by-products (e.g., aminoboranes, borazine) along with H_2.[2] For milder and controlled hydrogen release as well as for the preparation of B-N oligomers and polymers, many efforts have been dedicated to the study of the catalytic dehydrogenation and dehydropolymerization of this molecule and related primary NH_2RBH_3 and secondary NHR_2BH_3 amine–borane derivatives.[3] Within the wide variety of mechanisms proposed in the last decade, those based on s-block and early transition-metal systems involve intermediates with amidoborane $(NR_2BH_3)^-$ ligands.[3,4,5]

s-Block metal amidoborane compounds $[M(NH_2BH_3)_x]$ were initially evaluated as potentially improved solid-state alternatives to ammonia–borane for chemical hydrogen storage.[5] By using sterically demanding β-diketiminate ancillary ligands, Harder and co-workers prepared well-defined calcium and magnesium amidoborane complexes and explored their dehydrogenation in solution under mild conditions.[6] Hill and co-workers have intensively investigated Group 2 and 3 amidoborane complexes as catalysts and intermediates in amine–borane dehydrocoupling reactions.[7] In comparison, only a few Group 4 amidoborane complexes have been isolated, mainly supported within metallocene-type systems.[8] Interestingly, Manners and co-workers synthesized a paramagnetic titanium(III) amidoborane complex and suggested its key catalytic role in the dehydrogenation of amine-boranes by titanocene systems.[9]

We became interested in the study of stoichiometric reactions of half-sandwich Group 4 complexes $[MCp^*X_3]$ (M = Ti, Zr, Hf; $Cp^* = \eta^5\text{-}C_5Me_5$; X = CH_2SiMe_3, NMe_2) with amine–borane adducts as a synthetic route to hydride derivatives.[10] Multimetallic

3

low-valent titanium polyhydride complexes have revealed a great potential for the activation and cleavage of inert molecules such as dinitrogen, benzene, pyridines and quinolines at room temperature.[11] In particular, our group has recently reported the isolation of the low-valent titanium trinuclear hydride complex [{TiCp*(μ-H)}$_3$(μ$_3$-H)(μ$_3$-NMe$_2$BH$_2$)] (**1**) in the reaction of [TiCp*(CH$_2$SiMe$_3$)$_3$] with excess NHMe$_2$BH$_3$.[10b] Compound **1** contains a dimethylaminoborane fragment bridging three titanium atoms (Scheme 1) and represents a rare example where unstable NR$_2$BH$_2$ units can be trapped within a metal complex.[12] Herein we describe unprecedented BN ligands (NH$_2$BH$_2$NHBH$_3$)$^{2-}$ and {N(BH$_3$)$_3$}$^{3-}$ stabilized at bi- and trimetallic titanium(III) systems.

The treatment of [TiCp*Me$_3$] with 3 equiv. of NH$_3$BH$_3$ in toluene at ambient temperature afforded the dinuclear titanium(III) complex [{TiCp*(NH$_2$BH$_3$)}$_2$(μ-NH$_2$BH$_2$NHBH$_3$)] (**2**) (Scheme 1). Compound **2** was isolated in 70% yield as an extremely air-sensitive violet solid which is poorly soluble in hexane and moderately soluble in benzene and toluene.
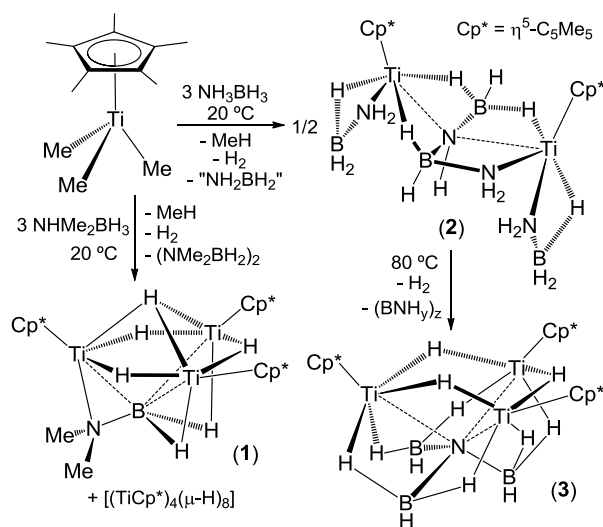
Scheme 1. Reaction of [TiCp*Me$_3$] with NHR$_2$BH$_3$ (R = H, Me).

The ^{1}H NMR spectrum of **2** in [D$_6$]benzene displays two downfield and broad resonance signals in a 1:1 ratio at δ = 29.5 ($\Delta\nu_{1/2}$ = 552 Hz) and 21.4 ($\Delta\nu_{1/2}$ = 376 Hz) ppm attributable to the η^5-C$_5$Me$_5$ ligands (Figure S6 in the Supporting Information). Complex **2** exhibits a good solubility in [D$_5$]pyridine or [D$_8$]tetrahydrofuran, and remains unaltered in those polar organic solvents at room temperature according to ^{1}H NMR spectroscopy. Nevertheless, the reaction of [TiCp*Me$_3$] with NH$_3$BH$_3$ in tetrahydrofuran leads to the isolation of **2** in low yield (15%), presumably due to the formation of other titanium by-products. Indeed, monitoring by ^{1}H NMR spectroscopy the reaction course in [D$_8$]tetrahydrofuran at room temperature revealed two broad resonance signals for **2** at δ = 29.2 ($\Delta\nu_{1/2}$ = 394 Hz) and 21.7 ($\Delta\nu_{1/2}$ = 275 Hz) ppm, those assigned to CH$_4$ and H$_2$, along with several resonances for unidentified species. It appears that the reaction of [TiCp*Me$_3$] with NH$_3$BH$_3$ may undergo variable routes depending on the reaction conditions. For instance, the analogous reaction of [TiCp*Me$_3$] with NH$_2$$t$BuBH$_3$ (3 equiv.) in toluene at room temperature gave a brown-purple oil containing titanium paramagnetic derivatives as determined by the absence of resonance signals in the ^{1}H NMR spectra. Crystallization in hexane at –35 ºC led to a small fraction (11%) of dark-blue crystals formed by the same number of titanium(III) monomeric amidoborane species [TiCp*(κ^2N,H-NHtBuBH$_3$)$_2$] and [TiCp*(κ^2N,H-NHtBuBH$_3$)(κ^3N,H,H-NHtBuBH$_2$Me)] in the asymmetric unit (Figure S2 and Tables S5 and S6 in the Supporting Information).[13] While the former component of the crystal could be related to a putative [TiCp*(NH$_2$BH$_3$)$_2$]$_x$ (x = 1 or 2) intermediate in the formation of **2**, the latter monomeric species contains one κ^3N,H,H-NHtBuBH$_2$Me ligand presumably formed by insertion of an aminoborane H$_2$B=NHtBu into a Ti–C bond.[7c,d]

The paramagnetic nature of **2** was confirmed by an Evans method determination of its magnetic susceptibility (μ_{eff} = 2.46 μ_B, 20 °C, C_5D_5N solution), which is in good agreement with the theoretical spin-only value (2.45 μ_B) for two non-interacting spins S = 1/2 in a dinuclear titanium(III) complex. The crystal structure of **2** shows two {TiCp*(NH_2BH_3)} units held together by a bridging $NH_2BH_2NHBH_3$ ligand (Figure 1). Each κ^2N,H-NH_2BH_3 ligand coordinates to the titanium atom through one Ti–N bond (Ti(1)–N(1) = 2.125(4) Å and Ti(2)–N(2) = 2.136(4) Å) and one Ti$\cdots$H–B interaction (Ti(1)$\cdots$B(1) = 2.508(5) Å and Ti(2)$\cdots$B(2) = 2.520(5) Å). These Ti–N and Ti$\cdots$B distances compare well with the analogous determined in the titanium(III) amidoborane complex [Ti(η^5-C_5H_5)$_2$(NH_2BH_3)] (2.153(3) and 2.520(4) Å, respectively).[8b] The μ-$NH_2BH_2NHBH_3$ ligand bridges asymmetrically between the metal centers. Thus, this moiety is bonded to titanium(1) by the N(4) atom (Ti(1)–N(4) = 2.216(3) Å), one Ti$\cdots$H–B interaction with the BH_3 group (Ti(1)$\cdots$B(4) 2.492(5) Å), and one Ti$\cdots$H–B interaction with the BH_2 group (Ti(1)$\cdots$B(3) 2.501(5) Å). The bridging ligand is also bonded to titanium(2) through the N(3) atom (Ti(2)–N(3) = 2.192(4) Å), the N(4) atom (Ti(2)–N(4) = 2.369(3) Å), and one Ti$\cdots$H–B interaction with the BH_3 group (Ti(2)$\cdots$B(4) 2.517(5) Å). Thus, each titanium exhibits a distorted octahedral geometry with the pentamethylcyclopentadienyl ligand and the N(4) atom occupying *trans* positions. Interestingly, the N(4) atom shows a rare five-coordinate environment and adopts a polyhedral geometry between square pyramidal and trigonal bipyramidal (τ_5 = 0.28).[14] Thus, the N(4) atom is in a plane with the B(3), B(4) and H(4) atoms (sum of angles about N(4) of 360°), while the Ti(1)–N(4)–Ti(2) angle is 141.4(2)°. The bridging ligand (H_2N-BH_2-NH-BH_3)$^{2-}$ in complex **2** is unprecedented in BN compounds, although it has been postulated as intermediate in the formation of dehydrogenated species (HN-BH-NH-BH_3)$^{2-}$

bridging two calcium centers.[5,6] Structurally documented ligands of the general form [(R)N-BH-N(R)-BH$_3$]$^{2-}$ (R = H, Me, iPr) in calcium and magnesium complexes contain short, intermediate and long B–N bond lengths.[6] In contrast, the B–N distances within the (NH$_2$BH$_2$NHBH$_3$) fragment of **2** are all in a narrow range from 1.524(7) Å to 1.548(6) Å, which is similar to those of the amidoborane $\kappa^2 N,H$-NH$_2$BH$_3$ ligands. This (H$_2$N-BH$_2$-NH-BH$_3$)$^{2-}$ motif may be envisioned as the doubly deprotonated form of the linear diborazane H$_3$N-BH$_2$-NH$_2$-BH$_3$, the product of a single dehydrocoupling reaction between two NH$_3$BH$_3$ molecules.[15]
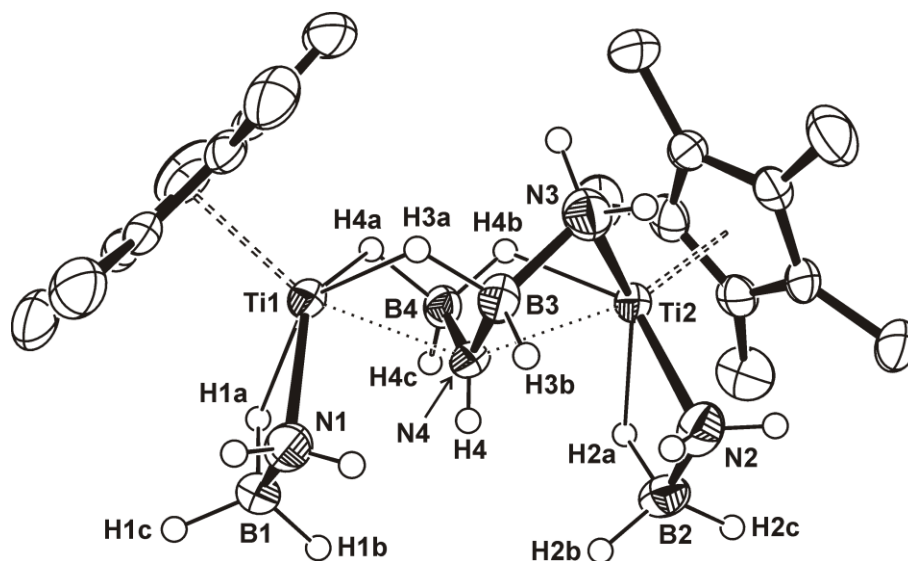

Figure 1. Perspective view of complex **2** (thermal ellipsoids at the 50% probability level). Hydrogen atoms of the η^5-C$_5$Me$_5$ ligand are omitted for clarity. Selected lengths (Å) and angles (º): Ti(1)–N(1) 2.125(4), Ti(1)–N(4) 2.216(3), Ti(2)–N(2) 2.136(4), Ti(2)–N(3) 2.192(4), Ti(2)–N(4) 2.369(3), B–N 1.524(7)–1.548(6), Ti⋯B 2.492(5)–2.520(5), Ti(1)–N(4)–Ti(2) 141.4(2), B(3)–N(4)–B(4) 124.5(4), N(3)–B(3)–N(4) 109.5(4).

A density functional theory (DFT) study was conducted to establish the electronic structure of the paramagnetic complex **2**. The computed geometry is in good agreement

with the crystallographic data (see Table S2 in the Supporting Information). The analysis of the electronic structure indicates that the unpaired electrons are localized on the titanium atoms in a parallel arrangement, which corresponds to a triplet state in agreement with the magnetic measurements. The shape of the two singly occupied molecular orbitals (SOMOs) of **2** is consistent with titanium d orbitals (Figure S3) and confirms that the oxidation state of the titanium atoms should be regarded as +3. Slightly lower in energy there are molecular orbitals which may be described as a bonding combination of a N(4) p orbital with smaller contributions of d orbitals of the two titanium atoms (Figure 2a). Natural Bond Orbital (NBO) analysis reveals the occupation of the N(4) orbitals, which are consistent with sp^2 hybridization for the nitrogen, while the remaining p orbital contains ≈1.5 e⁻ and interacts with empty d orbitals of the titanium centers.
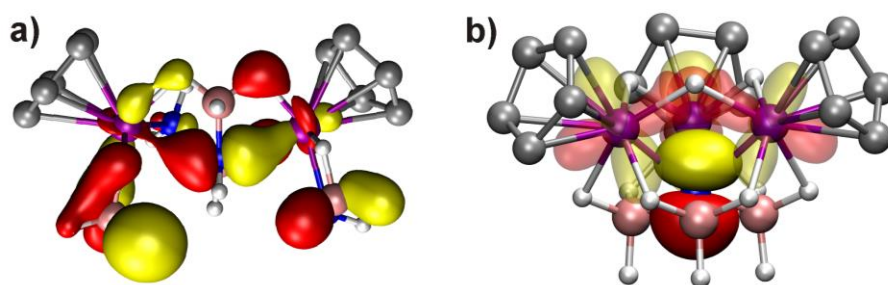

Figure 2. a) 3D representation of the MO for compound **2** showing the interaction of N(4) with both titanium atoms; b) NBO-determined orbital for compound **3** showing the donor-acceptor interaction of N(1) with the three titanium atoms (Color code: C = gray. H = white, Ti = purple, N = blue, B = pink). Methyl groups of the η^5-C₅Me₅ ligands are omitted for clarity.

Complex **2** is stable in [D₆]benzene or [D₈]tetrahydrofuran solutions at room temperature but readily decomposes at 80 ºC. The ¹H NMR spectrum of the resultant deep

red [D$_6$]benzene solution revealed the resonance signal for H$_2$ along with one broad resonance at δ = 12.5 (Δν$_{1/2}$ = 278 Hz) ppm. Similarly, the ^{1}H NMR spectrum of the thermal decomposition of **2** in [D$_8$]tetrahydrofuran showed a broad singlet at δ = 12.6 (Δν$_{1/2}$ = 241 Hz) ppm, whereas the ^{11}B NMR spectrum revealed resonance signals for borazine (BNH$_2$)$_3$ and polyborazylene (BNH$_y$)$_z$. In a preparative scale reaction, heating of **2** in tetrahydrofuran at 80 ℃ led to the isolation of deep red crystals of the trinuclear hydride complex [{TiCp*(μ-H)}$_3${μ$_3$-N(BH$_3$)$_3$}] (**3**) (Scheme 1). The ^{1}H NMR spectra of **3** are consistent with the C_{3v} symmetric structure determined in the solid-state structure (vide infra) and shows the single broad signal attributable to the equivalent η^5-C$_5$Me$_5$ ligands (Figure S7). The paramagnetic nature of **3** was confirmed by an Evans method determination of its magnetic susceptibility (μ$_{eff}$ = 2.35 μ$_B$, 20 ℃, C$_6$D$_6$ solution). Although resonance signals for the {μ$_3$-N(BH$_3$)$_3$} ligand were not detected in the ^{1}H NMR spectra, the IR spectrum (KBr) of **3** is very simple and shows one strong absorption at 2459 cm^{-1} for ν$_{BH}$ vibrations of terminal B-H bonds and one strong absorption at 2117 cm^{-1} for ν$_{BH}$ vibrations of bridging B-H groups (Figure S10).

While the ^{1}H NMR spectrum of the crude solid obtained in the thermal decomposition of **2** showed only the broad resonance for **3**, elemental analyses revealed a nitrogen content (10-12%) which is significantly higher than the expected value for **3** (2.30%). Furthermore, in addition to the bands due to complex **3**, the IR spectrum (KBr) of this solid shows two absorptions at 3444 cm^{-1} and 2502 cm^{-1} for ν$_{NH}$ and ν$_{BH}$ vibrations of terminal B-H bonds, respectively (Figure S11). This appears to be indicative of the formation of polyborazylene (BNH$_y$)$_z$ species with a solubility in organic solvents similar to that of complex **3**.[16] Compound **3** could be isolated as deep red crystals in 34% yield after successive crystallizations from hot hexane solutions.

The crystal structure of **3** shows three titanium atoms forming an equilateral triangle (Ti–Ti separations of 3.033(2) Å), wherein each edge of the triangle is bridged by one μ-H hydride ligand (Ti(1)–H(11) 1.85(7) Å) (Figure 3). Molecules of **3** present a C_3 axis which crosses the N(1) atom and is perpendicular to the Ti$_3$ plane. One face of the triangle contains a {μ$_3$-(κ^2*H*,*H*-H$_3$B)$_3$N} ligand with each BH$_3$ fragment bridging two titanium atoms through two Ti···H–B interactions (Ti(1)···B(1) 2.508(7) Å). The B(1)–N(1) bond length of 1.580(7) Å is longer than those found in amidoborane ligands and compares well with that determined in ammonia–borane (1.58(2) Å).[17] Therefore this value is indicative of B–N single bond and, along with the B–N–B angle of 109.8(3)º, suggests that the electron pair of nitrogen is shared with the titanium centers (Ti(1)–N(1) = 2.218(5) Å). Thus, the N(1) atom exhibits a distorted trigonal antiprismatic geometry (twist angle ϕ = 60º)[18] with Ti–N–Ti angles of 86.2(2)º. We have found no reference to the isolation of the {N(BH$_3$)$_3$}$^{3-}$ ligand or the neutral trisborylamine N(BH$_2$)$_3$ in the literature, although optimized structures have been analyzed by computational studies.[19] The related {NH$_2$(BH$_3$)$_2$}$^-$ motif was isolated as a sodium salt in the thermal rearrangement of [Na(NH$_2$BH$_3$)] and crystallographically characterized in the erbium complex [Er(H$_3$B–NH$_2$–BH$_3$)Cl$_2$(thf)$_3$] or, more recently, as the 18-crown-6 adduct [Na(18-crown-6)(thf)$_2$][NH$_2$(BH$_3$)$_2$].[20]
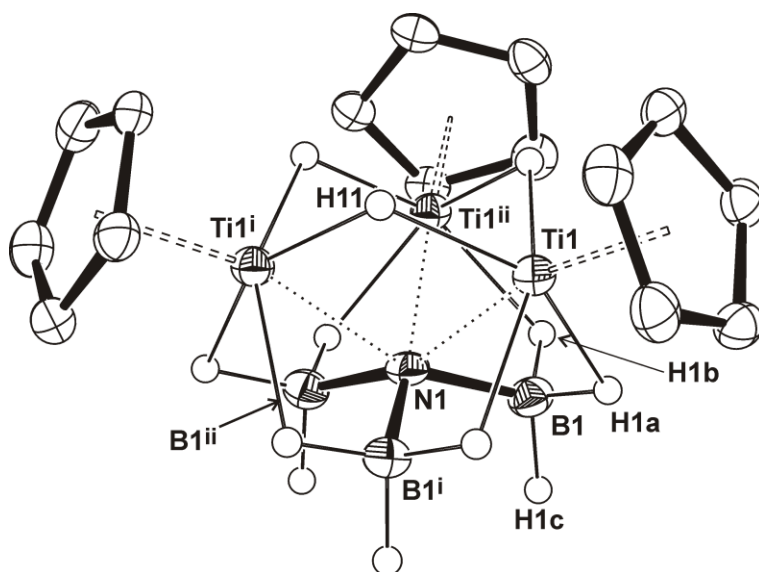
Figure 3. Perspective view of complex **3** (thermal ellipsoids at the 50% probability level). Methyl groups of the η^5-C_5Me_5 ligand are omitted for clarity. Selected lengths (Å) and angles (°): Ti(1)–N(1) 2.218(5), Ti(1)–H(11) 1.85(7), Ti(1)–H(1a) 2.02(7), Ti(1)–H(1b) 1.96(7), Ti(1)–Ti(1)^i 3.033(2), B(1)–N(1) 1.580(7), Ti(1)$\cdots$B(1) 2.508(7), Ti(1)–N(1)–Ti(1)^i 86.2(2), Ti(1)-N(1)-B(1) 80.7(3), B(1)–N(1)–B(1)^i 109.8(3). Symmetry code: (i) −x + y + 1, −x + 1, z; (ii) −y + 1, x − y, z.

The computed geometry (DFT) for a doublet ground state of **3** is in good agreement with the crystallographic data (Table S3). The analysis of the electronic structure of this species indicates that each titanium atom has one unpaired electron forming a spin frustrated system, where two electrons point up while the third one points down. While this situation does not agree with the magnetic measurements of μ_{eff} = 2.35 μ_B, the presence of a close excited quadruplet state of **3** ($\Delta E \approx 2$ kcal/mol) with a very similar geometry to the ground state might explain this value. The shape of the two SOMO orbitals of **3** is also consistent with single occupied titanium *d* orbitals (Figure S4) and confirms that the oxidation state of the titanium atoms should be regarded as +3. The NBO analysis shows

one bonding electron pair on N(1) with ca. 1.5 e⁻ interacting with empty d orbitals of the three titanium atoms (Figure 2b).

The structure of complex **3** resembles that reported by us for the analogous trinuclear tetrahydride species [{TiCp*(μ-H)}$_3$(μ_3-H)(μ_3-NMe$_2$BH$_2$)] (**1**) (Figure S1).[10b] A mixture of **1** and the tetranuclear octahydride [(TiCp*)$_4$(μ-H)$_8$][10b] was also obtained in the treatment of [TiCp*Me$_3$] with 3 equiv. of NHMe$_2$BH$_3$ (Scheme 1). While we previously described **1** as a mixed valence Ti(II)/Ti(III) complex based on the total negative charges (7–) of the η^5-C$_5$Me$_5$ and μ_n-H ligands, we have now studied its electronic structure by DFT calculations. The geometry of this compound can be also reproduced by the calculations as a spin-frustrated doublet ground state (Table S4 and Figure S5) in a similar fashion to **3**. These indicate that the titanium atoms of compound **1** are in the +3 oxidation state, which is consistent with the experimental μ_{eff} value of 1.87 μ_B at room temperature.[10b] Other optimizations, starting with a description of this compound as a mixed valence Ti(II)/Ti(III) species did not finish properly or produced higher energy species. The NBO analysis reveals that the N(1) atom has an electron pair with 1.7 e⁻ interacting with an empty d orbital of the Ti(2) atom (Figure 4a). In addition, the NBO analysis also shows bonding interactions between the three titanium atoms and the B(1) atom, which exhibits a certain extra electron density (0.7 e⁻) (Figure 4b). Thus, the six-coordinate geometry about the boron atom in **1** is distorted trigonal prismatic (twist angle ϕ = 0°).[18]
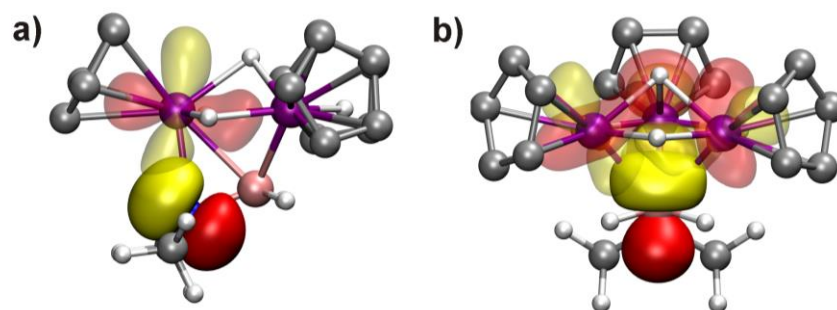
Figure 4. NBO-determined orbitals for compound **1**: a) shows the donor-acceptor interaction between N(1) and Ti(2), b) shows the interaction of B(1) with *d* orbitals of the three titanium atoms (Color code: C = gray. H = white, Ti = purple, N = blue, B = pink). Methyl groups of the η^5-C_5Me_5 ligands are omitted for clarity.

In summary, we have shown that anionic $(H_2N\text{-}BH_2\text{-}NH\text{-}BH_3)^{2-}$ and $\{N(BH_3)_3\}^{3-}$ fragments, which are not found in simple salts, can be stabilized as bridging ligands in titanium(III) complexes. The bimetallic amidoborane compound $[\{TiCp^*(NH_2BH_3)\}_2(\mu\text{-}NH_2BH_2NHBH_3)]$ was isolated in the reaction of ammonia–borane with the half-sandwich trimethyl complex $[TiCp^*Me_3]$, and its subsequent thermal treatment in solution afforded the trimetallic hydride derivative $[\{TiCp^*(\mu\text{-}H)\}_3\{\mu_3\text{-}N(BH_3)_3\}]$. In addition to the 3c,2e Ti···H–B interactions, these BN ligands and the analogous dimethylaminoborane trapped on $[\{TiCp^*(\mu\text{-}H)\}_3(\mu_3\text{-}H)(\mu_3\text{-}NMe_2BH_2)]$ exhibit bonding interactions of their N or B atoms with the titanium(III) centers. We are currently investigating the synthesis of multimetallic low-valent Group 4 compounds capable of stabilizing other unstable species.

Spanish Structures of Excellence María de Maeztu program through grant MDM-2017–0767.

Conflict of interest

The authors declare no conflict of interest.

References

[1]   a) T. B. Marder, *Angew. Chem. Int. Ed.* **2007**, *46*, 8116–8118; *Angew. Chem.* **2007**, *119*, 8262–8264; b) F. H. Stephens, V. Pons, R. T. Baker *Dalton Trans.* **2007**, 2613–2626; c) C. W. Hamilton, R. T. Baker, A. Staubitz, I. Manners, *Chem. Soc. Rev.* **2009**, *38*, 279–293.

[2]   a) A. Staubitz, A. P. M. Robertson, I. Manners, *Chem. Rev.* **2010**, *110*, 4079–4124; b) S. Frueh, R. Kellett, C. Mallery, T. Molter, W. S. Willis, C. King´ondu, S. L. Suib, *Inorg. Chem.* **2011**, *50*, 783–792.

[3]   a) H. C. Johnson, T. N. Hooper, A. S. Weller, *Top. Organomet. Chem.* **2015**, *49*, 153–220; b) A. Rossin, M. Peruzzini, *Chem. Rev.* **2016**, *116*, 8848–8872; c) A. L. Colebatch, A. S. Weller, *Chem. Eur. J.* **2019**, *25*, 1379–1390; d) D. Han, F. Anke, M. Trose, T. Beweries, *Coord. Chem. Rev.* **2019**, *380*, 260–286.

[4]   a) Y. Luo, K. Ohno, *Organometallics* **2007**, *26*, 3597–3600; b) M. E. Sloan, A. Staubitz, T. J. Clark, C. A. Russell, G. C. Lloyd-Jones, I. Manners, *J. Am. Chem. Soc.* **2010**, *132*, 3831–3841; c) M. Klahn, D. Hollmann, A. Spannenberg, A. Brückner, T. Beweries, *Dalton Trans.* **2015**, *44*, 12103-12111; d) M. Trose, M. Rei□, F. Rei□, F. Anke, A. Spannenberg, S. Boye, A. Lederer, P. Arndt, T. Beweries, *Dalton Trans.* **2018**, *47*, 12858–12862; e) T. Jurca, T. Dellermann, N. E. Stubbs, D. A. Resendiz-Lara, G. R. Whittell, I. Manners, *Chem. Sci.* **2018**, *9*, 3360–3366.

[5] T. E. Stennett, S. Harder, *Chem. Soc. Rev.* **2016**, *45*, 1112–1128.

[6] a) J. Spielmann, G. Jansen, H. Bandmann, S. Harder, *Angew. Chem. Int. Ed.* **2008**, *47*, 6290–6295; *Angew. Chem.* **2008**, *120*, 6386–6391; b) J. Spielmann, S. Harder, *J. Am. Chem. Soc.* **2009**, *131*, 5064–5065; c) J. Spielmann, D. F.-J. Piesik, S. Harder, *Chem. Eur. J.* **2010**, *16*, 8307–8318.

[7] a) D. J. Liptrot, M. S. Hill, M. F. Mahon, D. J. MacDougall, *Chem. Eur. J.* **2010**, *16*, 8508–8515; b) M. S. Hill, G. Kociok-Köhn, T. P. Robinson, *Chem. Commun.* **2010**, *46*, 7587-7589; c) P. Bellham, M. S. Hill, D. J. Liptrot, D. J. MacDougall, M. F. Mahon, *Chem. Commun.* **2011**, *47*, 9060–9062; d) P. Bellham, M. S. Hill, G. Kociok-Köhn, D. J. Liptrot, *Dalton Trans.* **2013**, *42*, 737–745.

[8] a) T. D. Forster, H. M. Tuononen, M. Parvez, R. Roesler, *J. Am. Chem. Soc.* **2009**, *131*, 6689–6691; b) D. J. Wolstenholme, K. T. Traboulsee, A. Decken, G. S. McGrady, *Organometallics* **2010**, *29*, 5769–5772; c) E. A. Jacobs, A. Fuller, S. J. Coles, G. A. Jones, G. J. Tizzard, J. A. Wright, S. J. Lancaster, *Chem. Eur. J.* **2012**, *18*, 8647–8658; for a nonmetallocene amidoborane complex, see: d) K. A. Erickson, J. P. W. Stelmach, N. T. Mucha, R. Waterman, *Organometallics* **2015**, *34*, 4693–4699.

[9] H. Helten, B. Dutta, J. R. Vance, M. E. Sloan, M. F. Haddow, S. Sproules, D. Collison, G. R. Whittell, G. C. Lloyd-Jones, I. Manners, *Angew. Chem. Int. Ed.* **2013**, *52*, 437–440; *Angew. Chem.* **2013**, *125*, 455–458.

[10] a) M. Greño, M. Mena, A. Pérez-Redondo, C. Yélamos, *Dalton Trans.* **2017**, *46*, 5138–5142; b) M. Greño, E. del Horno, M. Mena, A. Pérez-Redondo, V. Varela-Izquierdo, C. Yélamos, *Inorg. Chem.* **2017**, *56*, 11220–11229.

[11] a) T. Shima, S. Hu, G. Luo, X. Kang, Y. Luo, Z. Hou, *Science* **2013**, *340*, 1549–1552; b) S. Hu, T. Shima, Z. Hou, *Nature* **2014**, *512*, 413–415; c) S. Hu, G. Luo, T. Shima,

Y. Luo, Z. Hou, *Nature Comm.* **2017**, *8*, 1866; d) T. Shima, Z. Hou, *Top. Organomet. Chem.* **2017**, *60*, 23–43.

[12] a) G. Alcaraz, L. Vendier, E. Clot, S. Sabo-Etienne, *Angew. Chem. Int. Ed.* **2010**, *49*, 918–920; *Angew. Chem.* **2010**, *122*, 930–932; b) C. Y. Tang, A. L. Thompson, S. Aldridge, *Angew. Chem. Int. Ed.* **2010**, *49*, 921–925; *Angew. Chem.* **2010**, *122*, 933–937; c) P. Cui, T. P. Spaniol, L. Maron, J. Okuda, *Chem. Eur. J.* **2013**, *19*, 13437–13444; b) A. Kumar, N. A. Beattie, S. D. Pike, S. A. Macgregor, A. S. Weller, *Angew. Chem. Int. Ed.* **2016**, *55*, 6651–6656; *Angew. Chem.* **2016**, *128*, 6763–6768.

[13] CCDC 1885937-1885939 contain the supplementary crystallographic data for this paper. These data can be obtained free of charge from The Cambridge Crystallographic Data Centre.

[14] A. W. Addison, T. N. Rao, J. Reedijk, J. van Rijn, G. C. Verschoor, *J. Chem. Soc., Dalton Trans.* **1984**, 1349–1356.

[15] X. Chen, J.-C. Zhao, S. G. Shore, *J. Am. Chem. Soc.* **2010**, *132*, 10658–10659.

[16] a) P. J. Fazen, E. E. Remsen, J. S. Beck, P. J. Carroll, A. R. McGhie, L. G. Sneddon, *Chem. Mater.* **1995**, *7*, 1942–1956; b) J. Li, S. Bernard, V. Salles, C. Gervais, P. Miele, *Chem. Mater.* **2010**, *22*, 2010–2019.

[17] W. T. Klooster, T. F. Koetzle, P. E. M. Siegbahn, T. B. Richardson, R. H. Crabtree, *J. Am. Chem. Soc.* **1999**, *121*, 6337–6343.

[18] a) F. A. Cotton, G. Wilkinson, C. Murillo, M. Bochmann, *Advanced Inorganic Chemistry, 6th ed*, John Wiley & Sons, New York, 1999, pp. 6–7; b) S. El-Kurdi, K. Seppelt, *Chem. Eur. J.* **2011**, *17*, 3956–3962.

[19] a) A. F. Cuthbertson, C. Glidewell, *J. Mol. Struct. (THEOCHEM)* **1983**, *92*, 353–359; b) K.-A. Østby, A. Haaland, G. Gundersen, H. Nöth, *Organometallics* **2005**, *24*,

5318–5328; c) W. Shen, M. Li, Y. Li, S. Wang, *Inorg. Chim. Acta* **2007**, *360*, 619–624.

[20] a) S. R. Daly, B. J. Bellott, D. Y. Kim, G. S. Girolami, *J. Am. Chem. Soc.* **2010**, *132*, 7254–7255; b) H. Li, N. Ma, W. Meng, J. Gallucci, Y. Qiu, S. Li, Q. Zhao, J. Zhang, J.-C. Zhao, X. Chen, *J. Am. Chem. Soc.* **2015**, *137*, 12406–12414.